

Rapid Online Estimation of Time-Varying Thermal Boundary Conditions in Convective Heat Transfer Problem by ANN-Based Extended Kalman Smoothing Algorithm



Xinxin Zhang, Dike Li, Zeyuan Cheng, Jianqin Zhu, Zhi Tao, and Lu Qiu

Abstract In modern technologies, such as digital twin, it is essential to make real-time estimations of unknown time-varying boundary conditions from sensor measured data in given thermal systems, which leads to inverse heat transfer problems (IHTPs). However, due to the complexity of IHTPs, it's quite challenging to obtain a stabilized solution for online estimation with affordable computational cost. In this work, a rapid yet robust inversion algorithm called ANN-based extended Kalman smoothing algorithm is developed to realize the online estimation of unknown time-varying boundary conditions. Under the state-space representation of the extended Kalman smoothing algorithm, pre-trained fast ANN structures are deployed to replace the conventional CFD-based state transfer models, from which the computational process can be further accelerated by reducing the dimension of state variables. Two-dimensional tube convective heat transfer problem was employed as the case study to test the algorithm. The results show that the proposed algorithm is indeed a computational-light and anti-interference approach for solving IHTPs. The proposed algorithm can achieve estimation of unknown boundary conditions with a dimensionless average error of 0.0580 under noisy temperature measurement with a standard deviation of 10 K and its computational cost is reduced drastically compared with conventional approach from 12.23 s per time step to 3.506 ms.

Keywords Digital twin · Artificial neural network · Inverse problem · Kalman filter · Near real-time estimation

X. Zhang · D. Li · Z. Cheng · J. Zhu · Z. Tao · L. Qiu (✉)
Beihang University, Beijing 100191, PR China
e-mail: luqiu@buaa.edu.cn

1 Introduction

In many transient convective heat transfer problems, the unknown time-varying thermal boundary conditions (BCs) are difficult to be measured directly [1], yet whose online estimation is essential for improving the stability and performance of the thermal system in various engineering applications, such as aerospace thermal protection [2], chip cooling [3], metallurgical reactors [4, 5] and food engineering [6]. The inverse heat transfer problems (IHTPs) have been developed to estimate the unknown time-varying boundary conditions from the interior temperature fields. With the aid of the IHTP algorithm, it is possible to reconstruct the full temperature field as well as the thermal boundary condition from the online data measured by temperature sensors installed somewhere in the fluid domain. The technology is also known as digital twin.

However, the traditional methods to solve IHTPs faces the following challenges and drawbacks. Firstly, it is difficult to obtain relatively stable and accurate solutions under noisy input data due to the inherent ill-posedness of IHTPs [7], which means it is difficult to obtain relatively stable and accurate solutions under noisy input data. Secondly, it is difficult to invert the unknown heat flux from delayed sensor measurements since the thermal disturbance decays at the downstream due to the diffusive nature of heat transfer. Thirdly, the traditional algorithm to solve IHTPs is a computation-intensive and time-consuming process [8], which is difficult to be applied to online estimations.

The solutions for estimating time-varying BCs can be divided into two categories, namely, the whole domain algorithm and the sequential algorithm. The whole domain algorithm, by definition, is an offline method to calculate the unknown boundary conditions when all the time measurements in full time period are available. The algorithm transforms the IHTPs to an optimization problem, iteratively calculating the forward heat transfer process to minimize the error between the assumed and exact value of the unknown BCs by traditional optimization algorithms like Levenberg–Marquardt Method [9] or heuristic algorithms like repulsive particle swarm algorithm [10], ant colony optimization, and cuckoo search algorithm [11].

The sequential algorithms, on the other hand, work in the online mode. With continuously measured instantaneous temperature, the real-time or near real-time estimation of the unknown BCs can be achieved. Many sequential inversion methods have been brought up, including the sequential function specification method (SFSM) [12], dynamic matrix control method [13], multiple model adaptive inverse (MMAI) method [14], artificial neural network (ANN) algorithm [8, 15, 16], and digital filter (DF) approach [2, 4, 17–23], etc.

Beck [12] firstly introduced the concept of future measurement into IHTPs, which tackles the sensing delay issues to ensure a stabilized solution without time-lag or distortion. In order to reduce the interference caused by the noises, the digital filtering approach [2, 4, 17–23] are employed. Owing to its statistical trade-off between the sensor measurement and model prediction towards a smoothed result, the Kalman filtering approach is relatively more robust under noisy input data, which serves

as a valuable tool for tackling the ill-posed problem [7]. Scarpa and Milano [24] employed the Kalman filtering (KF) technique to solve a linear one-dimensional heat conduction problem, which shows the anti-interference ability of KF algorithms. The algorithm could be coupled with Rauch-Tung-Strieber (RTS) smoothing, which utilizes future time measurement to reduce the time lag in the prediction results. Although standard KF technique can be used to tackle linear IHTPs efficiently, it does not show pleasant for nonlinear IHTPs. Therefore, the extended version of Kalman filtering (EKF) technique [25], unscented Kalman smoothing algorithm [26], and other KF related methods [4, 17, 18, 21] are developed to deal with nonlinear IHTPs. Although the KF-related algorithms work well under noisy environment, but all of them share a common drawback, which is the prohibitively high computational cost caused by repetitive CFD forward calculations required in the sensitivity analysis.

Other algorithm, such as the artificial neural network (ANN) algorithm, with its powerful mapping ability [27] and high computational efficiency, may help to reduce computational cost. For instance, Najafi et al. [15, 16] utilized ANN models to directly correlate unknown BCs with sensor-measured temperatures, while Huang et al. [8] utilized well-trained ANN structures as the rapid forward solver, coupled with inverse algorithm, indirectly realizing the online estimation of unknown BCs. Both works demonstrate that the ANN algorithm could accelerate the computation of IHTPs with satisfactory accuracy. However, the major drawbacks of ANN algorithm are that, the training of ANN requires vast amount of dataset under high representation load, and it tends to overfitting when the sensor measurements are contaminated with noises.

To summarize, the KF-related approach is a robust method when measurement noise is non-negligible, but its high computational cost limits its applications towards online estimation task. The ANN models, on the other hand, as the universal approximators, could be employed to improve the computational efficiency of KF-related algorithm. Thus, in this work, we try to combine the extended Kalman smoothing algorithm and ANN algorithm to establish a rapid yet robust solution to IHTPs. Moreover, to reduce the redundant calculation of sensitivity analyzes requires in the traditional EKF approach, we developed a reduced form of EKF state vector with the aid of ANN model to further improve the computational efficiency. A two-dimensional convective heat transfer problem is selected as the case study for the implementation and evaluation of the proposed algorithm.

2 Inversion Procedure by Extended Kalman Smoothing

2.1 The Benchmark Problem

The case study is showed in Fig. 1, which describes a convective heat transfer problem on a two-dimensional rectangular region. A sensor is placed in the field, providing us with real-time temperature measurement while a time-varying heat flux, as the unknown BCs, is applied on the upper boundary. The main objective of our

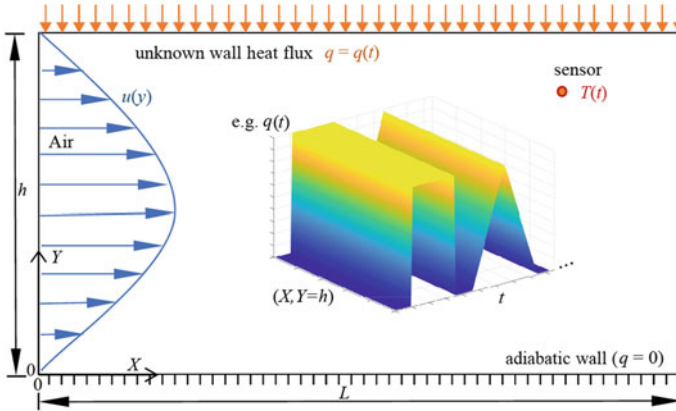


Fig. 1 The schematic of a 2D heat convection inverse problem

Table 1 Detailed parameters for the numerical example

Symbol	Quantity	Value
k_c	Coefficient of thermal conductivity	0.243 W/(m K)
ρ	Air density	1.29 kg/m ³
C_p	Specific heat capacity	1005 J/(kg K)
L	Length	1 m
h	Height	0.1 m

proposed algorithm is to estimate this unknown BCs in online mode by utilizing the continuously measured sensor temperatures.

The lower boundary is considered to be adiabatic. On the left boundary, fully developed air with an initial temperature $T_{in} = 300$ K and an average inlet velocity $u_m = 0.033$ m/s passes through the region. The default sensor location is (0.820, 0.089) and other detailed parameters are showed in Table 1.

Then, we give the governing equation for the above problem,

$$\rho C_p \frac{\partial T(X, Y, t)}{\partial t} + \rho C_p u(Y) \frac{\partial T(X, Y, t)}{\partial X} = k_c \frac{\partial^2 T(X, Y, t)}{\partial Y^2} \tag{1}$$

where the boundary conditions and initial conditions are

$$k_c \frac{\partial T(X, Y = h, t)}{\partial Y} = q(t) \tag{2}$$

$$k_c \frac{\partial T(X, Y = 0, t)}{\partial Y} = 0 \tag{3}$$

$$u(X = 0, Y, t) = u(Y) = 6u \left[\frac{Y}{h} \left(1 - \frac{Y}{h} \right) \right] \tag{4}$$

$$T(0, Y, t) = T_{in} \tag{5}$$

2.2 Extended Kalman Filtering

In this work, the IHTPs is solved by the ANN-based extended Kalman smoothing algorithm (ANN-EKS) which compose of two main parts, ANN-based forward solver and extended Kalman smoothing algorithm. The entire procedure is summarized as Fig. 2. The extended Kalman smoothing algorithm gives estimation of the unknown boundary conditions step by step and is accelerated based on the fast prediction of local temperature field and sensitivity analysis made by ANN-based forward solver.

The extended Kalman smoothing algorithm can be further separated into two sections, namely, the extended Kalman filtering (EKF) algorithm and the Rauch-Tung-Strieber (RTS) smoothing algorithm. The RTS smoothing algorithm enables the EKF algorithm to include future measurement into the estimation of unknown heat flux, which can address the sensing delay issue of IHTPs.

As aforementioned, the IHTPs is ill-posed by nature [7], which means small disturbance of the input data may cause large error in the output result. To solve this challenge, the extended Kalman filtering algorithm is employed, which uses the state-space representation to describe this two-dimensional convective heat transfer process and statistically quantifies the model error and the measuring noises. The algorithm compromises between the original prediction and the noisy measurements so that a more precise estimation could be made.

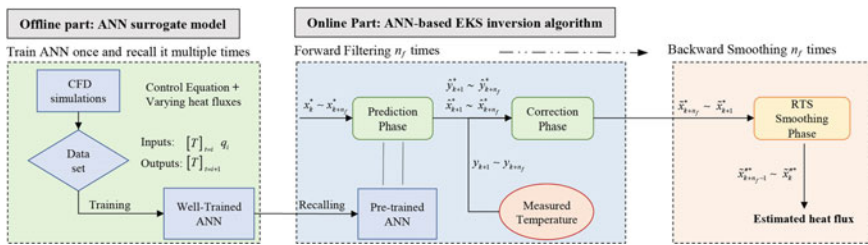


Fig. 2 The procedure of estimating time-varying heat flux at $t = k$ by the proposed algorithm

At first, the benchmark problem needs to be described under the state-space representation, whose nonlinear forms are respectively showed in Eqs. (6) and (7),

$$x_{k+1} = \Gamma(x_k, z_k) + \omega_{k+1} \quad (6)$$

$$y_{k+1} = \mathbf{H}(x_{k+1}) + v_{k+1} \quad (7)$$

where x is the state vector of the system describing its current state, y is the measurement vector, and z_k is the input of the system. The nonlinear operator Γ describes the dynamics of the system over time, and the nonlinear measurement operator \mathbf{H} maps the state vector to the measurement vector. The ω and v respectively are the state transfer model error and measurement noise, which are assumed to be independent zero-mean Gaussian noises with covariance matrix Q and R .

In order to apply the EKF algorithm for solving IHTPs, proper state variables need to be selected to fully describe the state of given thermal system. In literature [24–26], state vector x_k^* in the following form was employed,

$$x_k^* = [T_k^1 T_k^2 \dots T_k^i \dots T_k^N q_k]^T \quad (8)$$

where T_k^i ($i = 1, 2, \dots, N$) is the temperature of node i at time k , and N is the amount of mesh nodes used in the numerical computation of the benchmark problem, representing the temperature field in the discretized form. It is noteworthy that, the unknown boundary heat flux q_k , which was predicted and corrected with the EKF approach in each time step, was augmented into the state vectors in order to estimate the unknown heat flux.

In IHTPs, the measurement vector y is the sensor-measured temperature and the nonlinear measurement operator \mathbf{H} is then reduced to a linear matrix H showed as follows,

$$H = \begin{bmatrix} 0 & 0 & \dots & \underbrace{1}_{i=n_s} & \dots & 0 \end{bmatrix}_{1, N+1} \quad (9)$$

where the node index n_s corresponds to the sensor location in the temperature field.

The EKF approach estimates the next-time-step unknown boundary heat flux in two phases, the prediction phase and the correction phase.

In the prediction phase, the EKF approach predicts the unknown state vector as well as its probability distribution for the next-time step, which are realized by updating the means and covariance matrix of state vector x_{k+1}^* based on the current x_k^* and the following state space model,

$$x_{k+1}^* = \Gamma(x_k^*) + \omega_{k+1} \quad (10)$$

$$y_{k+1} = \mathbf{H}x_{k+1}^* + v_{k+1} \quad (11)$$

To calculate the means and covariance matrix of x_{k+1}^* , the EKF approach further linearize this problem by approximating $\Gamma(x_k^*)$ with first-order Taylor expansion at \tilde{x}_k^* ,

$$\Gamma(x_k^*) = \Gamma(\tilde{x}_k^*) + \left. \frac{\partial \Gamma}{\partial x_k^*} \right|_{x_k^* = \tilde{x}_k^*} (x_k^* - \tilde{x}_k^*) + o(x_k^* - \tilde{x}_k^*) \quad (12)$$

where \tilde{x}_k^* is the corrected estimation result at last time step k , and $\left. \frac{\partial \Gamma}{\partial x_k^*} \right|_{x_k^* = \tilde{x}_k^*}$ is the Jacobi matrix of the state vector, denoted as F_k ,

$$F_k = \left. \frac{\partial \Gamma}{\partial x_k^*} \right|_{x_k^* = \tilde{x}_k^*} = \begin{bmatrix} \frac{\partial \Gamma_1}{\partial x_{k,1}^*} & \cdots & \frac{\partial \Gamma_1}{\partial x_{k,N+1}^*} \\ \vdots & \vdots & \vdots \\ \frac{\partial \Gamma_{N+1}}{\partial x_{k,1}^*} & \cdots & \frac{\partial \Gamma_{N+1}}{\partial x_{k,N+1}^*} \end{bmatrix}_{(N+1) \times (N+1)} \quad (13)$$

It can be numerically calculated by the following means,

$$\frac{\partial \Gamma_i}{\partial x_{k,j}^*} \approx \frac{\Gamma_i(x_k^* + e_j \varepsilon x_{k,j}^*) - \Gamma_i(x_k^* - e_j \varepsilon x_{k,j}^*)}{2 \varepsilon x_{k,j}^*} \quad (14)$$

where $e_j = \left[0 \ 0 \ \cdots \ \underbrace{1^*}_j \ \cdots \ 0 \right]_{N+1}^T$ and $\varepsilon = 10^{-4}$.

Therefore, the final predicted results \hat{x}_{k+1}^* (means of x_{k+1}^*) and its error covariance matrix P_{k+1} are given below,

$$\hat{x}_{k+1}^* = \Gamma(\tilde{x}_k^*) \quad (15)$$

$$\hat{y}_{k+1}^* = H \hat{x}_{k+1}^* \quad (16)$$

$$P_{k+1} = F_k P_k' F_k^T + Q \quad (17)$$

where \hat{y}_{k+1}^* are the predicted measurement temperature at time step $k + 1$ and P' is the corrected error covariance matrix at time step k .

In the correction phase, the Kalman gain is calculated as follows, which can be considered as the confidence level ratio between the model prediction and sensor measurements.

$$K' = P_{k+1} H^T (H P_{k+1} H^T + R)^{-1} \quad (18)$$

Then the estimation results and the covariance matrix are corrected using the Kalman gain.

$$\tilde{x}_{k+1}^* = \hat{x}_k^* + K'(y_{k+1} - H\hat{x}_{k+1}^*) \tag{19}$$

$$P'_{k+1} = P_k - K'H_k P_k \tag{20}$$

2.3 RTS Smoothing

The EKF approach is a real-time inversion algorithm, which utilizes the current available data to estimate the unknown boundary heat flux. However, due to the diffusive nature of heat transfer process, the thermal response at sensor location lags behind the changing boundary heat flux, which is difficult to be captured by EKF approach itself.

In this work, a fixed interval smoothing algorithm called the Rauch-Tung-Strieber (RTS) smoothing technique is employed to include the data of future time measurement into the algorithm for better estimations.

As showed in Fig. 3, the RTS algorithm loops Kalman filtering procedures forwardly by n_f times and then slides back by n_f times to obtain a smoothed result. In the forward filtering procedures, we have already calculated the predicted \hat{x}_k^* , the corrected estimation \tilde{x}_k^* , the corresponding predicted error covariance P_k , the corrected P'_k , and the Jacobi matrix F_k at time step $k(k = k_0 \dots k_0 + n_f)$. Thus, the backward recursion procedures can be proceeded as follows,

$$G_k = P'_k F_k^T (P_{k+1})^{-1} \tag{21}$$

$$\tilde{x}_k^{/**} = \tilde{x}_k^* + G_k(\tilde{x}_{k+1}^{/**} - \tilde{x}_{k+1}^*) \tag{22}$$

where $\tilde{x}_k^{/**}$ and $\tilde{x}_{k+1}^{/**}$ are the smoothed results at time step $k, k + 1$ and G_k represents the RTS version of Kalman gain.

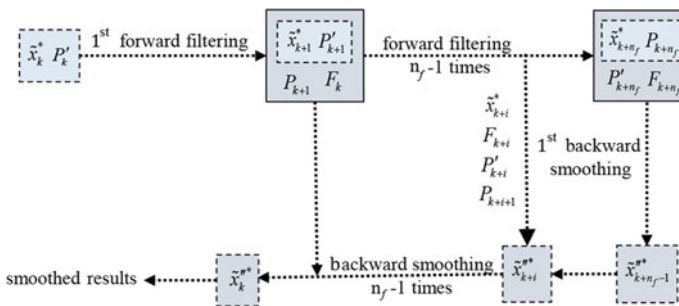


Fig. 3 The procedure of RTS smoothing at time step k

3 The ANN-Based Rapid State Transfer Model

In traditional KF-related approaches, the state transfer is usually achieved by CFD simulations, whose computation may take longer than the physical time in complex flow and heat transfer problems, thus being unsuitable for online inversion.

Alternatively, the artificial neural network is employed as a surrogate model for temperature field prediction by CFD, which can significantly reduce computational cost while holds certain level of accuracy [27].

More importantly, given that the ANN prediction does not require the information of entire temperature field, it allows to reduce the dimension of state vector in the EKS algorithm, which can tremendously reduce the computational cost and eventually realize online predictions.

3.1 The General Form of ANN-Based State Transfer Model

The key model in EKS algorithm is the state transfer model, which is composed of two parts. The first part approximates the next time step heat flux from step k to step $k + 1$ as showed in Eq. (23)

$$q_{k+1} = q_k + \omega_q \tag{23}$$

where we consider the induced error by this approximation as a part of the noise ω applied to the state transfer model. The second part forwardly calculates the next-time-step temperature field based on current temperature field and heat flux, which is achieved by ANN model. The input of ANN is the current state vector $x_k^* = [T_k^1 T_k^2 \dots T_k^i \dots T_k^N q_k]^T$, and the output is the next-time-step temperature field $T_{k+1} = [T_{k+1}^1 T_{k+1}^2 \dots T_{k+1}^i \dots T_{k+1}^N]^T$.

Despite the proven feasibility of this chosen state vector [24–26], the computational cost is still prohibitively expensive for online estimations. Large amounts of redundant sensitivity analysis are generated from this high-dimensional state vector containing the entire temperature field of all mesh nodes.

To address this problem, a novel state transfer model of reduced dimension is designed here with the aid of ANN algorithm. The reduced form of state vector is as follows,

$$x_k^* = [T_k^{n_s} T_k^{n_s+a} T_k^{n_s-a} T_k^{n_s+b} T_k^{n_s+b} q_k]^T \tag{24}$$

where the temperature value of sensor location $T_k^{n_s}$ is listed on the state vector along with the temperatures of four other points close to the sensor.

Then, the structure of ANN surrogate model should be organized as follows,

$$\text{Inputs: } [T_k^{n_s} \ T_k^{n_s+a} \ T_k^{n_s-a} \ T_k^{n_s+b} \ T_k^{n_s+b} \ q_k]^T \tag{25}$$

$$\text{Outputs: } [T_{k+1}^{n_s} \ T_{k+1}^{n_s+a} \ T_{k+1}^{n_s-a} \ T_{k+1}^{n_s+b} \ T_{k+1}^{n_s+b}]^T \tag{26}$$

3.2 The Generation of Dataset and the Training Procedure of ANNs

To train the ANN models, large amounts of numerical simulations are conducted to generate the training dataset.

The transient temperature field are calculated by solving the covering equations described in Sect. 2.1 with finite volume method, which applies upwind differential scheme in x direction, central differential scheme in y direction, and the implicit scheme is adopted for the time marching [11]. The total mesh size is 25×50 with $\Delta x = 0.04$ m and $\Delta y = 0.002$ m.

To cover a variety of changing thermal boundary conditions on the heated wall, as shown in Fig. 4, a series of heat flux evolutions were adopted such as step functions, polynomial functions, sinusoid waves and triangular waves in different amplitudes and frequencies, which will generate rich state transfer information for the training of ANN models. Moreover, the training dataset could be furthered expanded by applying Eq. (14) during the above simulation, so as to simulate the sensitivity analysis by elevating and lowering one of the state variable's value and then calculating the next-time results.

Therefore, the final training heat flux, with a total times steps of 6794 (time duration of 67.94 s on the testing computer), is applied to the benchmark problem including the four above forms of heat fluxes showed in Fig. 4 with different amplitudes and frequencies. The CFD predicted temperature field is then reorganized into the standard form of inputs and outputs of ANN for training purpose.

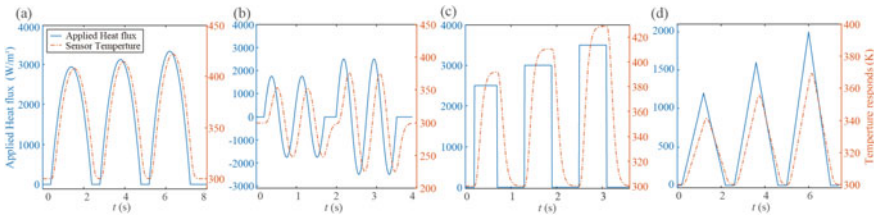


Fig. 4 The schematic of generating dataset by applying various form of heat flux and obtaining temperature distribution over time. **a** Step heat flux. **b** Triangular heat flux. **c** Parabolic heat flux. **d** Sinusoid heat flux

The final dataset includes state transfer data needed in Eq. (10) as well as the sensitivity analysis data needed in Eq. (14). However, the data volume of the former is only 1/12 of the latter. The unbalanced dataset may cause the ANN model fitting more closely to the pattern of sensitivity analysis but works poorly under state transfer scenario. To resolve this unbalanced dataset problem, we choose to divide the dataset and train two ANN models used for state transfer prediction and sensitivity analysis respectively. Therefore, 6794 sets of data are used for training the state transfer ANN model and the remaining 81,529 sets of data are used for training the sensitivity ANN model.

The fully connected multi-layer perception (MLP) neural network is chosen in this work. Both ANN models compose of three layers, with 10 neurons in the hidden layer. The inputs and outputs are standardized in order to enhance training performance. The hyperbolic tangent (tanh) function is chosen as the active function and the Levenberg–Marquardt backpropagation algorithm is used to train the neural network. The training procedure of ANN model for state transfer prediction ends after 1422 iterations when the performance of the network stops improving in the validation dataset for 6 consecutive epochs. To validate the training method, datasets are randomly divided into three parts, 70% of which are used for training, 15% for validation and 15% for testing respectively. The pre-trained neural network eventually achieves a mean square error of 7.14×10^{-9} in the testing dataset and the regression R value reaches 0.99999, while the training procedure of ANN model for sensitivity analysis ends after 552 iterations and achieves a mean square error of 8.02×10^{-9} in the testing dataset and the regression R value reaches 0.99997, indicating that the training is successful and the obtained neural network can meet the accuracy criterion for surrogating the state transfer models.

4 Results and Discussions

4.1 Verification on the Feasibility of the Proposed Algorithm and Discussions

In order to test the feasibility of the proposed algorithm, a transient CFD simulation is performed, in which the heat flux on the upper wall is varying in the manner showed in Fig. 5 (solid line). The CFD predicted temperature variation at the point (x, y) , is then extracted to simulate the temperature measurements with a sensor.

Given that the sensor-measured temperature is inevitably contaminated with noises, a zero-mean Gaussian noise ($\sigma \sim N(0, 1)$) with a noise level m is imposed on the simulated temperature evolution at the point (x, y) to simulate the noisy measurements y_k ,

$$y_k = T_k + m\sigma. \quad (27)$$

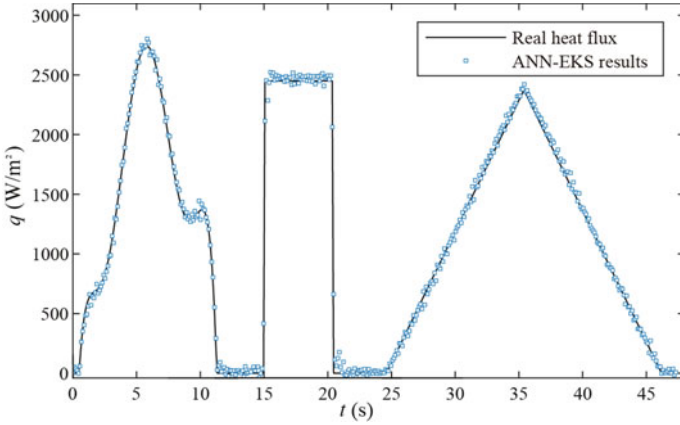


Fig. 5 Comparison between the real heat flux and the estimation results under noise level $m = 2$ (Plot interval: every 11 time steps)

where T_k is the simulated real temperature value at sensor location of time step k .

In this test, the noise level is set to be $m = 2$. Feeding the artificial measurements y_k into the ANN-EKS algorithm as the input, one can get the output q_k . Figure 5 compares q_k with the wall thermal boundary condition used in the CFD simulation q''_k , which could be treated as the “true” value. The results show that the predicted heat flux evolution agrees well with the “true” value, indicating the ANN-EKS based IHTPs solver works well to predict the historical thermal boundary condition that varied with complex wave functions, such as step function, a triangular wave and an arbitrary smooth curve.

To evaluate the algorithm’s performance quantitatively, the average error (AE) is defined to describe the accuracy of the estimation results,

$$AE = \sqrt{\frac{1}{n} \sum_{k=1}^n (\bar{q}''_k - \bar{q}_k)^2} \tag{28}$$

where the \bar{q}''_k and \bar{q}_k are the dimensionless form of applied heat flux and estimation results and n is the number of total time steps.

And the average computing time per time step is defined to evaluate the computational efficiency of our algorithm. All the simulations involved in this work are performed on a personal computer with 2.50 GHz Intel (R) Core (TM) i7-11700F processor and 32 GB of RAM.

4.2 Comparison Study with Other Algorithms

In order to highlight the advantage of the proposed algorithm, it is compared with the inverse ANN algorithm [15, 16] and the extended Kalman smoothing algorithm (EKS) [24, 25].

The inverse ANN algorithm [15, 16] mainly utilizes the artificial neural network model to directly map the sensor-measured temperature to the unknown boundary conditions. The inputs of the ANN model are the past and future temperature measurement $[T_{k+n_p} \dots T_{k-1} T_k T_{k+1} \dots T_{k+n_f}]^T$ at the sensor locations, and the outputs are the boundary heat flux $[q_k]$ in the current time step. The inverse ANN algorithm possesses high computational efficiency due to its direct ANN-aided prediction of unknown BCs from the sensor measurements, but it may tend to overfitting and performs poorly when the measurement noises are relatively high.

The extended Kalman smoothing algorithm [24, 25] employs the full form of the state vector, the transfer of which is calculated based on the traditional CFD methods. Though this algorithm copes well under noisy measurement, the redundant sensitivity analysis, caused by the high-dimensionality of the full-form state vector, lead to tremendously high computational cost and limits its applications toward online estimations.

It can be seen that the proposed algorithm has a lower accuracy than the traditional inverse ANN algorithm under relatively lower noise level. However, it outperforms the inverse ANN algorithm when the noise level is higher than 10, indicating that the proposed algorithm works robustly under noisy input data. Moreover, the *AE* of the proposed algorithm is close to that of the CFD-based EKS algorithm, which proves that the simplification of our work in the state vector is reasonable.

Notably, Fig. 6 shows the inversion results of the above three algorithm (scatter) against the testing heat flux (solid line) under a relatively high noise level of $m = 10$. The results of our ANN-EKS algorithm and traditional EKS algorithm match the real heat flux well with an *AE* of 0.0580 and 0.0609 respectively while the inverse ANN algorithm seemingly oscillates greatly under this high noise level and performs the worst with an *AE* of 0.0825. Also, we can notice that the proposed ANN-EKS algorithm possesses better ability to suppress overshooting and oscillation of the prediction compared with the other two methods, which further proves the robustness of our algorithm in noisy environments.

More importantly, our proposed algorithm also has great advantages in terms of computational efficiency. our ANN-EKS algorithm can drastically reduce the computational time of the conventional EKS approach from 11.3 s per time step to 5.43 ms in the comparison study. Since the primary goal of our algorithm is online estimation, we set a criterion to evaluate the algorithm's online ability, which is the computing time per time step should not exceed the computational time interval (0.01 s in this case). Judged by the criterion for online estimation, 5.43 ms is significantly shorter than the time step interval of 0.01 s, which means our algorithm is fully capable of performing online estimation task while the conventional EKS approach cannot.

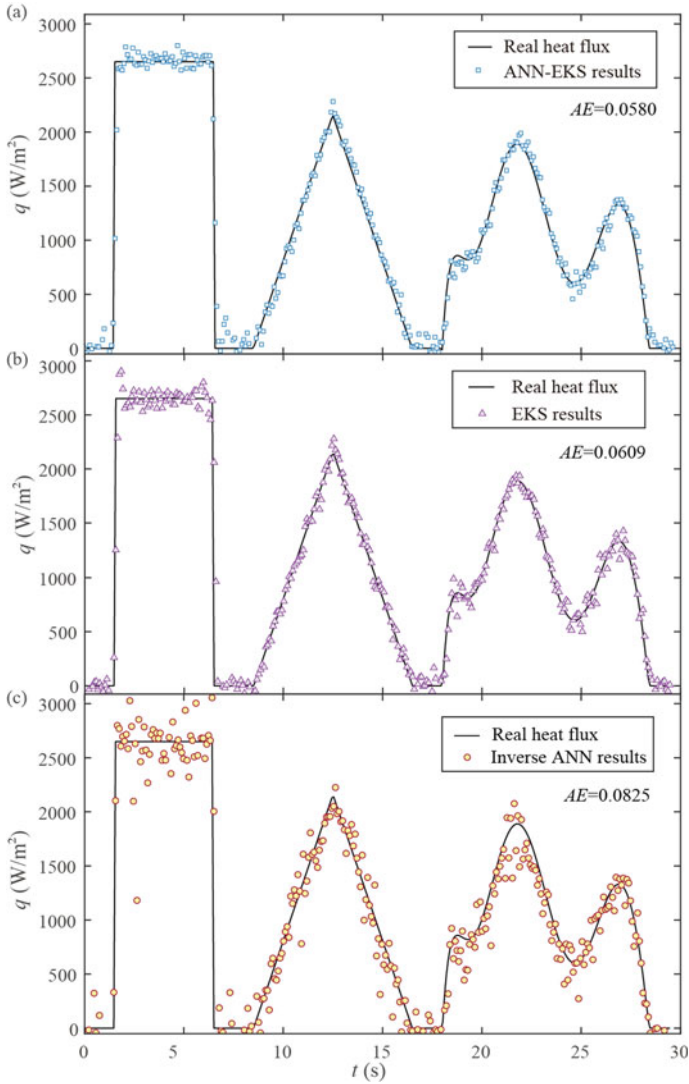


Fig. 6 The estimation results of the three algorithms under noise level $m = 10$ k (Plot interval: every 9 time steps). **a** The ANN-based EKS results with $AE = 0.0580$. **b** The EKS results with $AE = 0.0609$. **c** The inverse ANN results with $AE = 0.0825$

Based on the comparison results, it is safe to say that our proposed algorithm is indeed a robust and rapid approach and capable of achieving online estimation task for solving IHTPs.

5 Conclusion

A rapid yet robust inversion algorithm, ANN-based extended Kalman smoothing algorithm, is developed to realize the online estimation of time-varying thermal boundary conditions in a two-dimensional tube convective heat transfer problem. The major findings are summarized as follows:

1. The proposed algorithm is a computational-light online approach for the estimation of the unknown boundary conditions. Compared with conventional CFD-based EKS algorithm, the computational costs of the proposed are reduced drastically from 11.3 s per time step to 5.31 ms, which makes our algorithm fully capable of performing online estimation task.
2. The proposed algorithm is relatively robust to handle measurement data with high noise-signal ratio. An average error of 0.0580 for estimating unknown boundary heat flux can be achieved via our algorithm, whose accuracy is basically equivalent to the conventional EKS algorithm with an average error of 0.0609 and improves significantly compared to the inverse ANN algorithm with an average error of 0.0825.

References

1. Ku, C.Y., Liu, C.Y., Xiao, J.E., Hsu, S.M., Yeih, W.: A collocation method with space-time radial polynomials for inverse heat conduction problems. *Eng. Anal. Boundary Elem.* **122**, 117–131 (2021)
2. Uyanna, O., Najafi, H., Rajendra, B.: An inverse method for real-time estimation of aerothermal heating for thermal protection systems of space vehicles. *Int. J. Heat Mass Transf.* **177**(2), 121482 (2021)
3. Jang, H.-Y., Cheng, C.-H.: Nonlinear optimal on-line heat-dissipation control methodology in electronic devices. *Int. J. Heat Mass Transf.* **52**(7), 2049–2058 (2009)
4. LeBreux, M., Désilets, M., Lacroix, M.: An unscented Kalman filter inverse heat transfer method for the prediction of the ledge thickness inside high-temperature metallurgical reactors. *Int. J. Heat Mass Transf.* **57**(1), 265–273 (2013)
5. Wang, G., et al.: Fuzzy identification of the time- and space-dependent internal surface heat flux of slab continuous casting mold. *J. Heat Transf.* **140**(12) (2018)
6. Białobrzeski, I.: Determination of the heat transfer coefficient by inverse problem formulation during celery root drying. *J. Food Eng.* **74**(3), 383–391 (2006)
7. Alifanov, O.M.: *Inverse Heat Transfer Problems* (1994)
8. Huang, S., et al.: On-line heat flux estimation of a nonlinear heat conduction system with complex geometry using a sequential inverse method and artificial neural network. *Int. J. Heat Mass Transf.* **143** (2019)
9. Golsorkhi, N.A., Tehrani, H.A.: Levenberg-marquardt method for solving the inverse heat transfer problems (2014)
10. Lee, K.H.: Application of repulsive particle swarm optimization for inverse heat conduction problem—parameter estimations of unknown plane heat source. *Int. J. Heat Mass Transf.* **137**, 268–279 (2019)
11. Udayraj, et al.: Performance analysis and feasibility study of ant colony optimization, particle swarm optimization and cuckoo search algorithms for inverse heat transfer problems. *Int. J. Heat Mass Transf.* **89**, 359–378 (2015)

12. Beck, J.V.: Nonlinear estimation applied to the nonlinear inverse heat conduction problem. *Int. J. Heat Mass Transf.* **13**(4), 703–716 (1970)
13. Li, Y., Wang, G., Chen, H.: Simultaneously regular inversion of unsteady heating boundary conditions based on dynamic matrix control. *Int. J. Therm. Sci.* **88**, 148–157 (2015)
14. Wang, G., et al.: A multiple model adaptive inverse method for nonlinear heat transfer system with temperature-dependent thermophysical properties. *Int. J. Heat Mass Transf.* **118**, 847–856 (2018)
15. Najafi, H., Uyanna, O., Zhang, J.: Application of artificial neural network as a near-real time technique for solving non-linear inverse heat conduction problems in a one-dimensional medium with moving boundary. In: *Proceedings of the ASME 2020 Summer Heat Transfer Conference* (2020)
16. Najafi, H., Woodbury, K.A.: Online heat flux estimation using artificial neural network as a digital filter approach. *Int. J. Heat Mass Transf.* **91**, 808–817 (2015)
17. Daouas, N., Radhouani, M.S.: A new approach of the Kalman filter using future temperature measurements for nonlinear inverse heat conduction problems. *Numer. Heat Transf. Part B Fundam.* **45**(6), 565–585 (2004)
18. Wen, S., et al.: Application of KF-RLSE algorithm for on-line estimating the time-dependent melting thickness and input heat flux in participating media. *Int. J. Therm. Sci.* **125**, 1–10 (2018)
19. Ko, Y.-H., et al.: Inverse estimation problem of determining the unknown timewise-varying strength of a primer rapid heat source. *Procedia Eng.* **79**, 295–304 (2014)
20. Wen, S., et al.: An on-line extended Kalman filtering technique for reconstructing the transient heat flux and temperature field in two-dimensional participating media. *Int. J. Thermal Sci.* **148** (2020)
21. Wen, S., et al.: Real-time estimation of time-dependent imposed heat flux in graded index media by KF-RLSE algorithm. *Appl. Therm. Eng.* **150**, 1–10 (2019)
22. da Silva, W.B., et al.: Sequential particle filter estimation of a time-dependent heat transfer coefficient in a multidimensional nonlinear inverse heat conduction problem. *Appl. Math. Model.* **89**, 654–668 (2021)
23. Jahangiri, A., Mohammadi, S., Akbari, M.: Modeling the one-dimensional inverse heat transfer problem using a Haar wavelet collocation approach. *Physica A* **525**, 13–26 (2019)
24. Scarpa, F., Milano, G.: Kalman smoothing technique applied to the inverse heat conduction problem. *Numer. Heat Transf. Part B Fundam.* **28**(1), 79–96 (1995)
25. Gaaloul, N., Daouas, N.: An extended approach of a Kalman smoothing technique applied to a transient nonlinear two-dimensional inverse heat conduction problem. *Int. J. Therm. Sci.* **134**, 224–241 (2018)
26. Wen, S., et al.: Simultaneous estimation of internal temperature field and boundary time-dependent heat flux in absorbing and scattering media using the unscented Kalman smoothing technique. *J. Quant. Spectrosc. Radiat. Transf.* **255** (2020)
27. Hornik, K., Stinchcombe, M., White, H.: Multilayer feedforward networks are universal approximators. *Neural Netw.* **2**(5), 359–366 (1989)